USGS
science for a changing world

A One-Dimensional Model of Solid-Earth Electrical Resistivity beneath Florida

By Cletus Blum, Jeffrey J. Love, Kolby Pedrie, Paul A. Bedrosian, and E. Joshua Rigler

Open-File Report 2015–1185

U.S. Department of the Interior
U.S. Geological Survey

U.S. Department of the Interior
SALLY JEWELL, Secretary

U.S. Geological Survey
Suzette M. Kimball, Acting Director

U.S. Geological Survey, Reston, Virginia: 2015

Contents

Figures

Conversion Factors

Inch/Pound to International System of Units

Multiply	By	To obtain
Length		
mile (mi)	1.609	kilometer (km)
foot (ft)	0.3048	meter (m)
inch (in.)	2.54	centimeter (cm)

Resistivity (ρ) in ohm $\cdot$meter (Ω•m) may be converted to conductivity (σ) in siemens per meter (S/m) as $\rho = \frac{1}{\sigma}$.

Abbreviations Used in this Report

1D	one dimensional
3D	three dimensional
FERC	Federal Energy Regulatory Commission
Hz	hertz
km	kilometer
m	meter
Ma	mega-annum
NERC	North American Electric Reliability Corporation
nT	nanotesla (magnetic field strength, one-billionth of a tesla)
S	siemens
S/m	siemens per meter
USGS	United States Geological Survey
mV	millivolts

Symbols

ρ_a	apparent resistivity
ω	angular frequency
σ	conductivity
>	greater than
<	less than
M Ω	megohm
Ω•m	ohm meter

A One-Dimensional Model of Solid-Earth Electrical Resistivity beneath Florida

By Cletus Blum, Jeffrey J. Love, Kolby Pedrie, Paul A. Bedrosian, and E. Joshua Rigler

Abstract

An estimated one-dimensional layered model of electrical resistivity beneath Florida was developed from published geological and geophysical information. The resistivity of each layer is represented by plausible upper and lower bounds as well as a geometric mean resistivity. Corresponding impedance transfer functions, Schmucker-Weidelt transfer functions, apparent resistivity, and phase responses are calculated for inducing geomagnetic frequencies ranging from 10^{-5} to 100 hertz. The resulting one-dimensional model and response functions can be used to make general estimates of time-varying electric fields associated with geomagnetic storms such as might represent induction hazards for electric-power grid operation. The plausible upper- and lower-bound resistivity structures show the uncertainty, giving a wide range of plausible time-varying electric fields.

Introduction

Geoelectric fields, induced in the Earth's conducting interior during magnetic storms, represent a natural hazard for the operation of electric-power grids (for example, Bolduc, 2002; Boteler, 2003). In response to the possible vulnerability of U.S. power grids, in May 2013, the Federal Energy Regulatory Commission of the Department of Energy issued FERC Order No. 779 directing the North American Electric Reliability Corporation (NERC-DOE, 2010) to develop power-grid standards to help mitigate the deleterious impact of storm-induced geoelectric fields. In support of these developments, the Geomagnetism Program of the U.S. Geological Survey (USGS) has assembled a simplified model of electrical resistivity beneath Florida, a part of the United States that was not specifically covered by an earlier effort undertaken by Fernberg (2012). This resistivity model for Florida contributes to a larger USGS and interagency U.S. Government project for evaluating induction hazards associated with geomagnetic storms (Love and others, 2014).

Method Summary

To develop a one-dimensional (1D), depth-dependent model of electrical resistivity for Florida, we first assemble a layered-earth structure sequence for the lithosphere (crust and upper mantle) beneath the tectonically distinct northern and southern parts of Florida. For a given rock type, electrical resistivity can differ by orders of magnitude depending on mineralogy, water content, chemistry, and degree of weathering. Therefore, for each of the northern and southern Florida layered-earth sequences, we assigned a range of resistivity values based on rock type and published results from geological and geophysical surveys and from direct laboratory measurements of standard rock types for each layer. A 1D model, applicable to all of Florida, has a set of layers and resistivity values that encompass the

separate northern and southern Florida layered-earth structures; a reference resistivity model is obtained by calculating the geometric mean from the resistivity range for each stratigraphic layer. Using the 1D model, we calculate impedance transfer functions, Schmucker-Weidelt transfer functions, and apparent resistivity and phase responses that describe the frequency-dependent relation between the induced geoelectric fields and the inducing geomagnetic field variation.

Tectonic and Geologic Overview

We begin by summarizing the complex tectonic and geological history of Florida (for review, see Lane, 1994). The basement rocks of Florida originate from the Gondwana supercontinent (570–180 Ma), a mosaic of continental blocks that is the ancestor of South America and Africa, and were amalgamated in the Early Cambrian period through several orogonies. During the Paleozoic and early Mesozoic tectonic assembly of Pangea (510–180 Ma), multiple collisions between Gondwana and Laurentia, the ancestor of North America, formed a mountain chain complex that included what is now the Appalachian Mountains. With the assembly of Pangea, the Suwannee Basin and Florida-Bahama blocks detached from Gondwana and attached to Laurentia (Hine, 2013), as shown in figure 1. The Suwannee block accumulated terrane fragments from Laurentia forming a composite-terrane block (Mueller and others, 2014). Subsequently, with the Mesozoic opening of the Atlantic (~170–70 Ma), extensional forces moved and stretched the Florida-Bahama block, creating a series of basins and arches accompanied by localized igneous intrusions. The divide between the older Suwanee block to the north and the younger Florida-Bahama block to the south is known as the Bahama fracture zone.
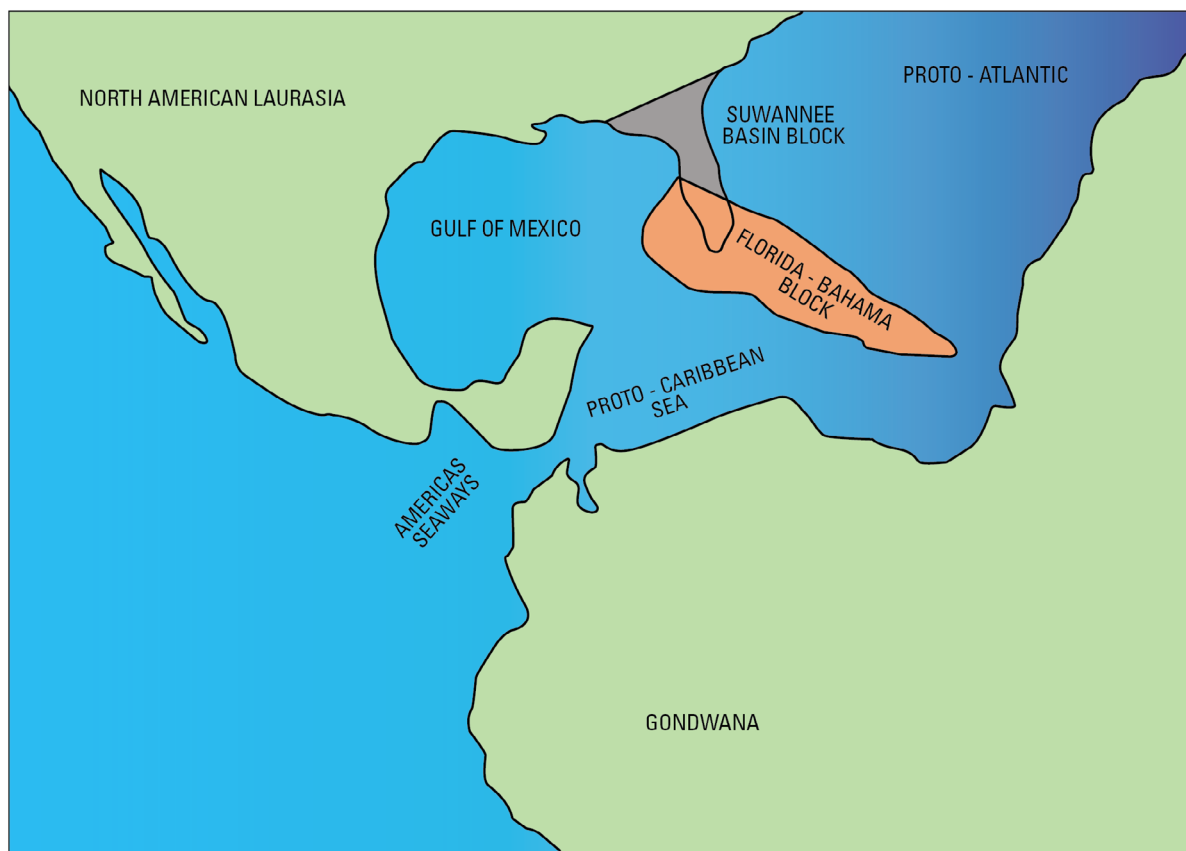

Figure 1.   Paleogeographic map depicting the final assembly of the Florida basement rocks. Modified from Hine, 2013, figure 3.4.
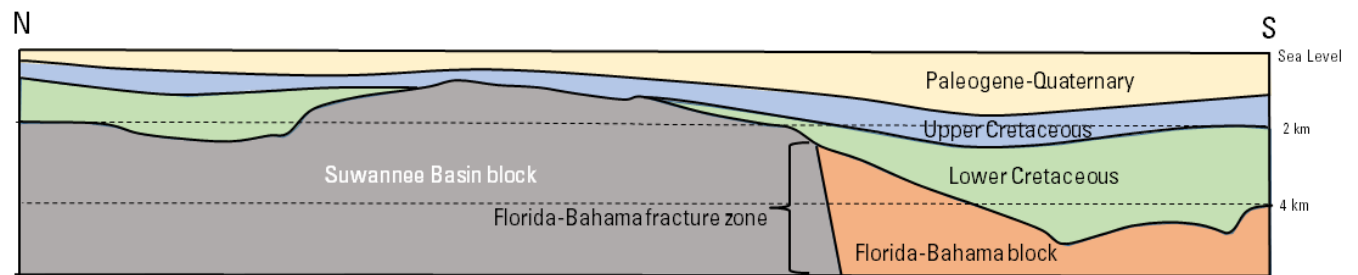
Figure 2. Geologic cross section showing the generalized basement structure of the Florida peninsula, modified from Barnett, 1975, figure 4, based on firsthand examination of subsurface samples and supplemented by well logs and literature. N, north; S, south; km, kilometer.

In the Late Jurassic (~160 Ma), substantial carbonate deposition began across the blocks of the Florida peninsula and continued almost uninterrupted into the late Paleogene (~30 Ma) (Hine, 2013); see figure 2. During this interval, Florida was beneath a warm, shallow ocean with carbonate deposition atop the basement accompanying fluctuations in sea level, as shown in figure 2. From the late Paleogene through the Neogene (~10 Ma), siliciclastic sediments shed from a second uplift of the Appalachian Mountains intermittently interrupted carbonate deposition (Hine, 2013). Both carbonate and siliciclastic sediments were deposited on the Florida peninsula from the Neogene to the Quaternary (Scott, 2001).

Northern and Southern Layered-Earth Structures

The preceding geological summary motivates our assembly of two Florida-based, layered-earth structural sequences on either side of the northwest-southeast trending Bahama fracture zone. Within the deep lithosphere and asthenosphere, both structural sequences are taken to be identical; they include the lower mantle, which for this project extends from 670- to 1,000-kilometers (km) depth, the mantle transition zone from 410- to 670-km depth, and an upper mantle from 40- to 410-km depth. An interpreted crustal thickness of 40 km is based on the Florida-to-Edmonton Broadband Seismometer Experiment (French and others, 2009). North of the Bahama fracture zone, late Precambrian igneous and metamorphic rocks (mostly granite) of the Suwannee block compose the basement and come to within 1 km of the surface (Barnett, 1975). South of the Bahama fracture zone, igneous and metamorphic rocks (granite with basaltic intrusions) of the Florida-Bahama block are known to characterize the basement deeper than 6 km (Smith, 1982). We assume that both the north and south basements are homogenous down to the base of the crust at 40-km depth. In the north, an early Paleozoic sedimentary sequence overlays igneous basement rocks (Barnett, 1975), while to the south, limestone and other carbonate rocks directly overlay the igneous and metamorphic basement (Hine, 2013).
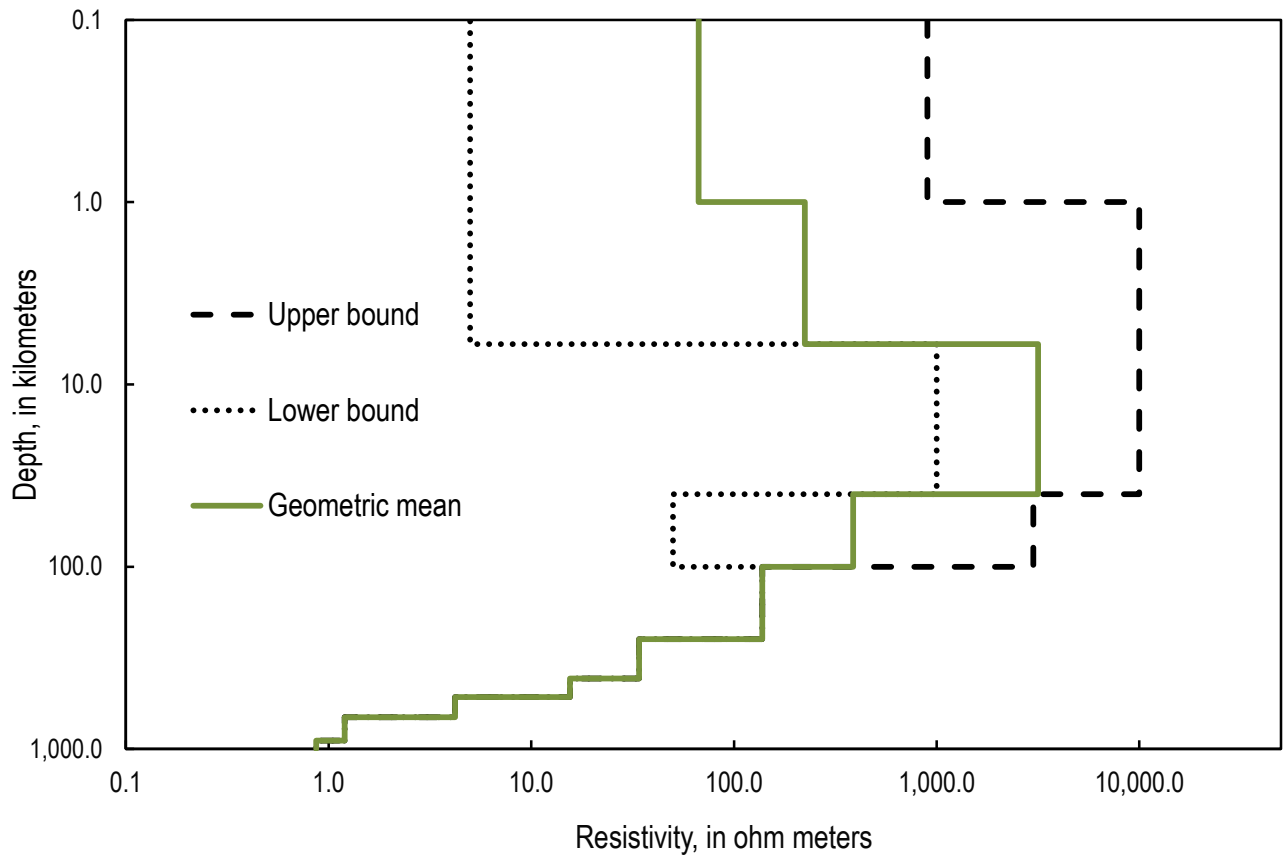
Figure 3. Resistivity-depth model for the Florida peninsula. Upper and lower resistivity bounds are shown with dashed and dotted black lines, respectively. The solid green line shows the geometric mean.

Resistivity versus Depth

In figure 3, we show the resistivity-depth model, including the upper bound, lower bound, and corresponding geometric mean resistivities versus depth; numerical values are given in tables 1–3 of the appendix and references therein. The upper, lower, and mean depth versus resistivity models are shown in figure 4. The layer structure of the upper model corresponds with the northern layer structure, and the layer structure of the lower model corresponds with the layer structure of the southern layer structure. Taking into consideration the northern and southern layered-earth structures and the upper and lower bounds of their resistivity values, the end members were chosen for the upper and lower bounds. In practice, given the northern and southern structures, the upper resistivity bound uses the resistivity values for each layer of the northern structure and the lower resistivity bound uses the lowest resistivity values of the southern structure. The geometric mean is calculated from the layer thicknesses and resistivity values of the upper and lower bounds.
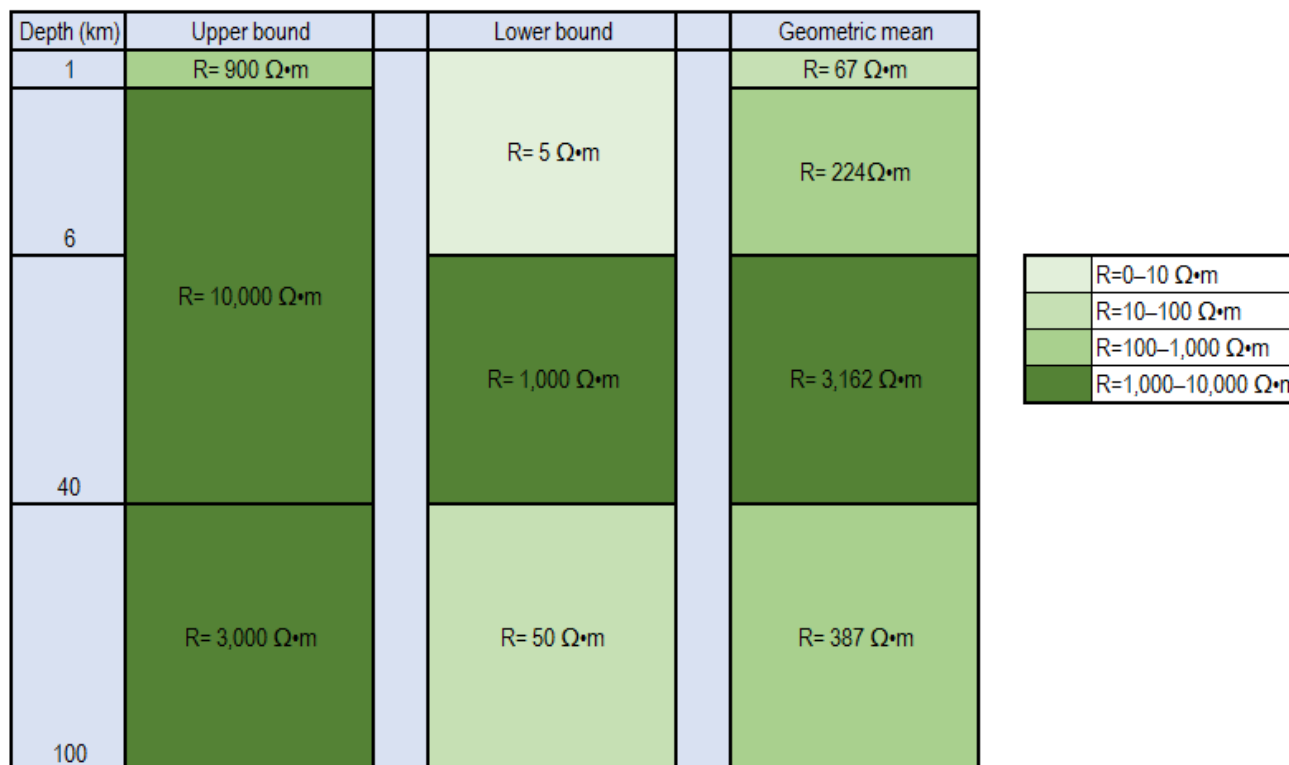
4

Figure 4. Layer thickness profile with resistivity values for all three models up to a 100-kilometer depth. Note depth values are not to scale. Ω•m, ohm meter; km, kilometer.

Sedimentary strata: Resistivity values are commonly reported corresponding to rock age as well as rock type. Published sedimentary rock resistivity values of similar type rocks and ages found in Florida range from 5 to 900 Ω•m (Keller and Frischknecht, 1966; Jones, 1999).

Crustal basement (<40-km depth): Resistivity values for early Paleozoic intrusive rocks typically range from 1,000 to 5,000 Ω•m, while Mesozoic extrusive rocks have resistivities ranging from 20 to 500 Ω•m (Keller, 1966). Specific resistivity values for rock types have been published, giving granite (intrusive rock) a resistivity value of 4,300 Ω•m and basalt (extrusive rock) of 800 Ω•m (Palacky, 1988). Generally speaking, published resistivity values for the upper crust range from 800 to 30,000 Ω•m, and lower-crustal resistivity values range from 8 to 200 Ω•m (Jones, 1999). Given the lithology of the basement rocks in Florida, a resistivity value of 10,000 Ω•m is used for the upper bound. For the lower bound, a low published resistivity value of 8 Ω•m (Keller, 1966) is used.

Upper mantle (40- to 410-km depth): Resistivity values for the upper mantle can be constrained from magnetotelluric surveys, with a wide range of values reported from different regions. Globally, the continental upper mantle has resistivity values ranging from 50 to 200 Ω•m, while oceanic upper mantle has significantly higher resistivity, on the order of 10^5 Ω•m (Jones, 1999). Two magnetotelluric surveys with transects across the Appalachian Mountains through the coastal plains (for example, Mareschal and others, 1983; Ogawa and others, 1996) report upper mantle resistivity ranging from 1,000 to 3,000 Ω•m. The upper-bound resistivity value is taken from these two surveys, whereas the lower-bound resistivity value of 50 Ω•m is based upon Jones 1999.

Lower mantle and mantle transition zone (410- to >1,000-km depth): The resistivity values for the mantle (100- to 1,000-km depth) are taken from a coarse global resistivity model by Kelbert and others (2009), which are based upon magnetic observatory data. The station closest to Florida that is used in Kelbert's analysis is the Stennis magnetic observatory, which is located at the John C. Stennis Space Center in Mississippi.

Transfer Functions

The preceding 1D resistivity model can be used to estimate the amplitude and direction of the geoelectric field induced at the Earth's surface by geomagnetic activity. This can be accomplished by calculating a frequency domain transfer function relating the induced geoelectric field and the inducing geomagnetic field (for example, Simpson and Bahr, 2005; Lordan, 2013).

The impedance tensor, **Z**, specifies the relation between the geoelectric field, **E**, in millivolts per kilometer (mV/km), and the magnetic intensity, **B**/μ, in amps per meter (A/m); here, μ is the magnetic permeability, assumed to be identical to the free space permeability. In the frequency domain,

E = **Z**·**B**/μ.

The Schmucker-Weidelt transfer function (Simpson and Bahr, 2005) **C** specifies the relation between the geoelectric field **E** and the time rate of change of the magnetic field, d**B**/dt, in nanoteslas per second (nT/s). In the frequency domain,

E = **C**· $i\omega$**B**,

where ω is angular frequency, measured in radians per second, and i is the square root of -1. For a 1D depth-dependent resistivity model (figs. 5 and 6), a frequency-dependent apparent resistivity, ρ_a, (fig. 7) can be calculated; it is related to the magnitude of **Z** as

ρ_a= |**Z**(ω)|^2 /(μω).

Impedance phase (Ø), usually plotted along with apparent resistivity (fig. 8), can be calculated as

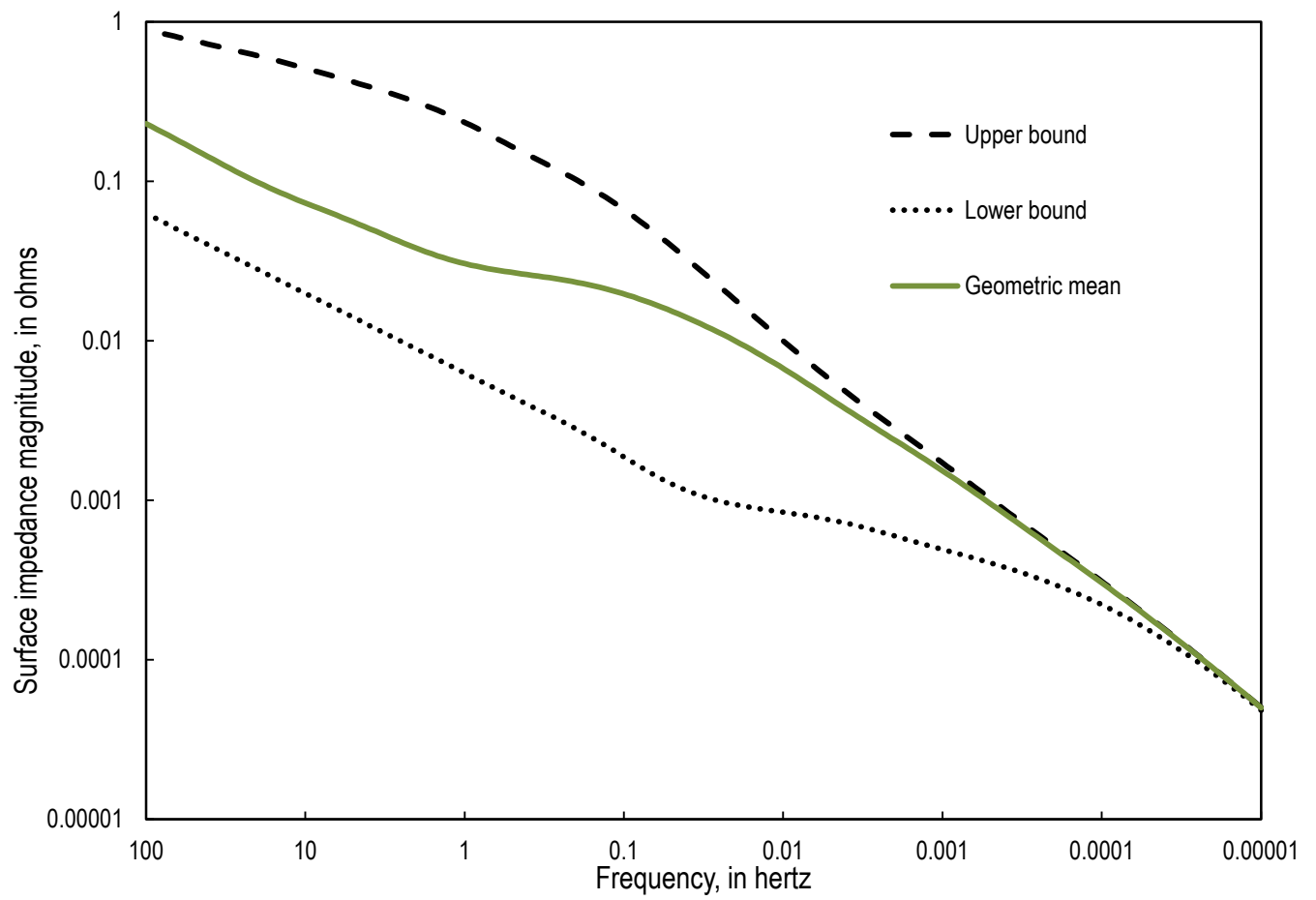$$\emptyset = tan^{-1}(\frac{E_x}{B_y}).$$

6

Figure 5.   Surface impedance magnitude versus frequency for the upper bound, lower bound, and geometric mean.
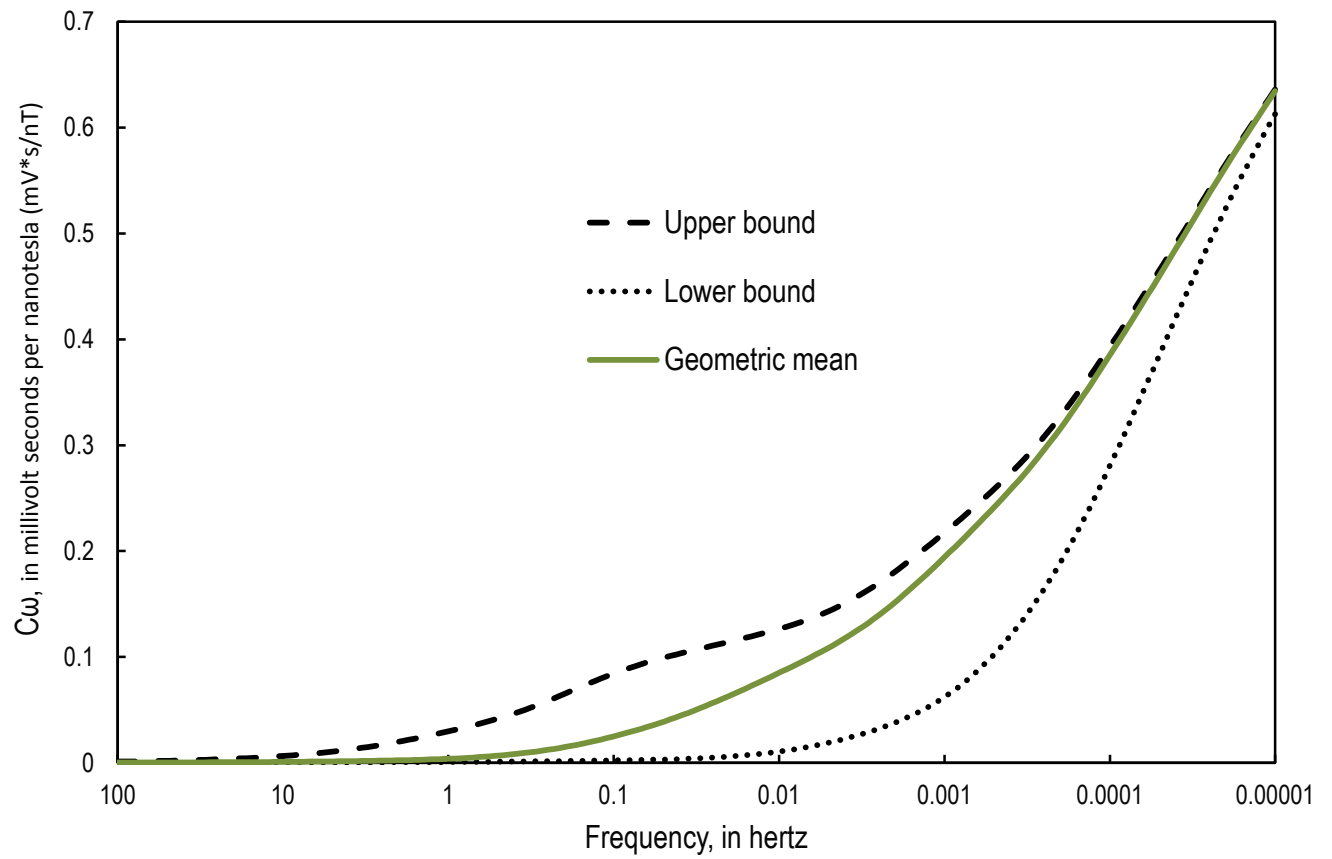
Figure 6. Schmucker-Weidelt transfer function magnitude versus frequency for the upper bound, lower bound, and geometric mean.
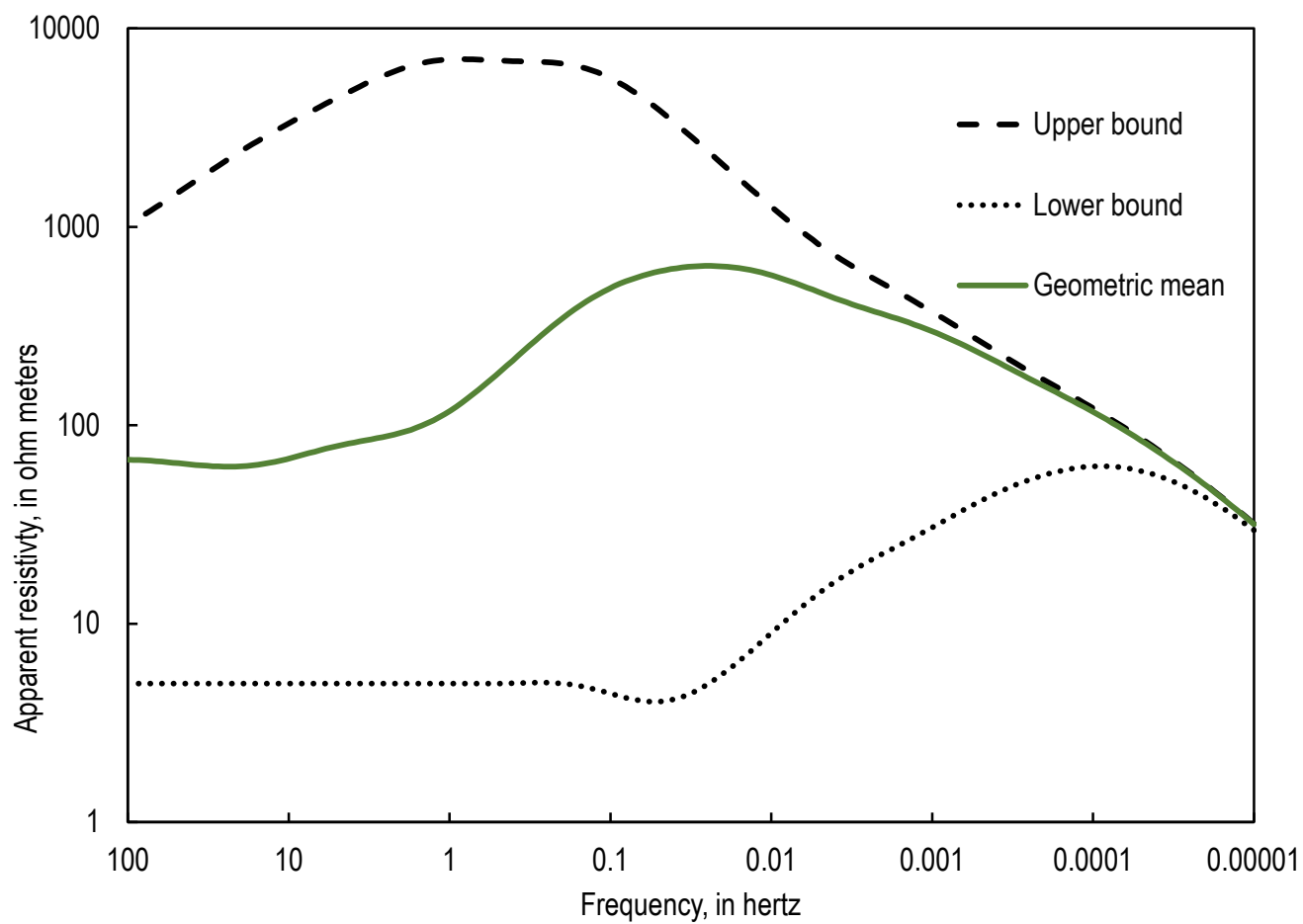
Figure 7. Apparent resistivity versus frequency for the upper bound, lower bound, and geometric mean.
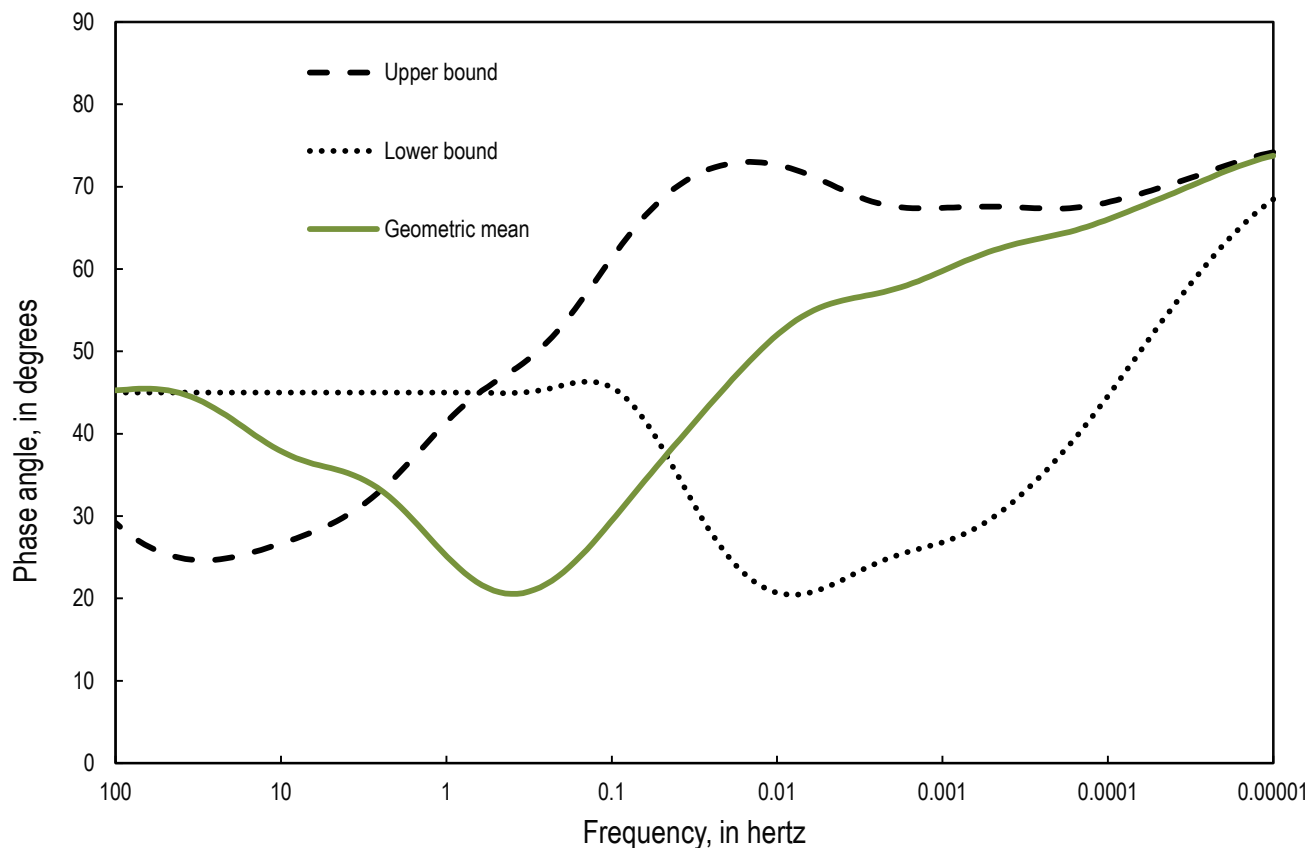
Figure 8. Phase angle versus frequency for the upper bound, lower bound, and geometric mean.

Discussion and Conclusions

The results of this study are limited by the lack of a detailed Florida-wide magnetotelluric survey. The EarthScope program of the National Science Foundation has supported a transportable array of magnetotelluric stations that have, so far, been deployed across the northwestern and midwestern United States (Schultz, 2009; http://www.earthscope.org). As part of that project, data have been inverted for regional three-dimensional (3D) resistivity models at lithospheric scales, revealing significant anisotropy in resistivity (for example, Patro and Egbert, 2008; Meqbel and others, 2012; Bedrosian and Feucht, 2014). Given Florida's complicated geologic and tectonic history, it is reasonable to expect that the crust and upper mantle have significant anisotropy in resistivity structure. Furthermore, the large resistivity contrast between the crust and the ocean can significantly distort the amplitude, direction, and phase of induced geoelectric fields. The complexity of these important effects is not captured using a one-dimensional (1D) resistivity model.

The USGS Geomagnetism Program recently completed a magnetotelluric survey of the Florida peninsula which can be used to model the 3D resistivity of Florida. The 1D model presented in this report can provide general geological and geophysical context for 3D modeling. It will be of interest to

compare the electromagnetic response functions from the 3D models with the corresponding response functions reported here for 1D resistivity, specifically noting directional heterogeneity. With respect to magnetic-storm induction hazards, it will be of interest to compare hypothetical storm-time geoelectric time series calculated using the impedance tensors of the 1D model with more accurate geoelectric time series calculated from the site-specific impedance tensors obtained from direct magnetotelluric measurement.

Acknowledgments

References Cited

Barnett, R.S., 1975, Basement structure of Florida and its tectonic implications: Gulf Coast Associations of Geological Society Transactions, v. 25, p. 122–142, accessed July 7, 2014, at http://archives.datapages.com/data/gcags/data/025/025001/0122.htm.

Bedrosian, P.A., and Feucht, D., 2014, Structure and tectonics of the northwestern United States from EarthScope USArray Magnetotelluric Data: Earth and Planetary Science Letters, v. 402, p. 275–289. [Also available at http://dx.doi.org/10.1016/j.epsl.2013.07.035.]

Bolduc, Léonard, 2002, GIC observations and studies in the hydro-Quebéc power system: Journal of Atmospheric and Solar-Terrestrial Physics, v. 64, no. 16, p. 1793–1802, accessed October 15, 2014, at http://www.sciencedirect.com/science/article/pii/S1364682602001281.

Boteler, D.H., 2003, Geomagnetic hazards to conducting networks: Natural Hazards, v. 28, no. 2, p. 537–561, accessed October 15, 2014, at http://link.springer.com/article/10.1023/A:1022902713136#page-1.

Fernberg, Peter, 2012, One-dimensional Earth resistivity models for selected areas of Continental United States and Alaska: Electric Power Research Institute (EPRI) Technical Update 1026430, accessed July 7, 2014, at http://jupiter.ethz.ch/~kuvshinov/For_Dima_Alexeev/150116_Relevant_Papers_for_Revision/1D_profiles_for_North_America.pdf.

French, S.W., Fischer, K. M. Syracuse, E. M. and Wysession, M. E., 2009. Crustal structure beneath the Florida-to-Edmonton broadband seismometer array: Geophysical Research Letters, v. 36, L08309, accessed July 7, 2014, at http://onlinelibrary.wiley.com/doi/10.1029/2008GL036331/full.

Hine, A.C., 2013, Geologic History of Florida: Gainesville, Florida, University Press of Florida, 256 p.,

Jones, A.G., 1999. Imaging the continental upper mantle using electromagnetic methods: Lithos, v. 48, nos. 1–4, p. 57–80, accessed October 15, 2014, at http://www.sciencedirect.com/science/article/pii/S0024493799000225.

Kelbert, Anna, Schultz, Adam and Egbert, Gary, 2009, Global electromagnetic induction constraints on transition-zone water content variations: Nature, v. 460, p. 1003–1006, accessed July 7, 2014, at http://www.nature.com/nature/journal/v460/n7258/abs/nature08257.html.

Keller G.V., and Frischknecht F.C., 1966, Electrical methods in geophysical prospecting: Oxford, United Kingdom, Pergamon Press, p. 46–52.

Lane, Ed, ed., 1994, Florida's geological history and geological resources: Florida Geological Survey Special Publication 35, 76 p., accessed July 7, 2014, at http://ufdc.ufl.edu/UF00000124/00001.

Lordan, R., 2013, How to calculate electric fields to determine geomagnetically-induced currents: Electric Power Research Institute, Technical Update, 3002002149, Palo Alto, California, 36 p., accessed October 15, 2014, at http://www.epri.com/abstracts/Pages/ProductAbstract.aspx?ProductId=000000003002002149&Mode=download.

Love, J.J., Rigler, E.J., Pulkkinen, A., and Balch, C.C., 2014, Magnetic storms and induction hazards, Eos, Transactions American Geophysical Union, v. 95, no. 48, 445–446 p., accessed October 15, 2014, at http://onlinelibrary.wiley.com/doi/10.1002/2014EO480001/full.

Mareschal, J-C., Musser, J., and Bailey, R.C., 1983, Geomagnetic variation studies in the southern Appalachians—Preliminary results: Canadian Journal of Earth Sciences, 1983, v. 20, no. 9, accessed July 7, 2014, at http://www.nrcresearchpress.com/doi/abs/10.1139/e83-129.

Meqbel, N., Egbert, G.D., Wannamaker, P.E., Kelbert, A. and Schultz, A., 2012, Deep electrical resistivity structure of the northwestern U.S. derived from 3-D inversion of USArray magnetotelluric

data: Earth and Planetary Science Letters, v. 402, p. 290–304, accessed July 7, 2014, at http://www.sciencedirect.com/science/article/pii/S0012821X13007413.

Mueller, P.A., Heatherington, A.L., Foster, D.A., Thomas, W.A. and Wooden, J.L., 2014, The Suwannee suture—Significance for Gondwana-Laurentia terrane transfer and formation of Pangaea: Gondwana Research, v. 26, no. 1, p. 365–373, accessed July 7, 2015, at http://www.sciencedirect.com/science/article/pii/S1342937X13002232.

NERC-DOE, 2010, High-impact, low-frequency event risk to the North American bulk power system: North American Electric Reliability Corp. and U.S. Department of Energy, accessed October 15, 2014, at http://www.nerc.com/pa/CI/Resources/Documents/HILF%20Report.pdf.

Ogawa, Y., Jones, A.G., Unsworth, M.J., Booker, J.R., Lu, A., Craven, J.C., Roberts, B., Parmalee, J., and Farquharson, C., 1996, Deep electrical conductivity structures of the Appalachian Orogen in the Southeastern U.S.: Geophysical Research Letters, v. 23, p. 1597–1600, accessed July 7, 2014, at http://onlinelibrary.wiley.com/doi/10.1029/95GL03601/full.

Palacky, G.J., 1988, Resistivity characteristics of geologic targets, *in* Nabighian, M.N., Electromagnetic methods in applied geophysics: Society of Exploration Geophysicists Investigation in Geophysics, v. 3, p. 53–129.

Patro, P.K. and Egbert, G.D., 2008, Regional conductivity structure of Cascadia—Preliminary results from 3D inversion of USArray transportable array magnetotelluric data: Geophysical Research Letters, v. 35, no. 20, accessed October 15, 2014, at http://onlinelibrary.wiley.com/doi/10.1029/2008GL035326/pdf.

Schultz, A., 2009, EMScope—A continental scale magnetotelluric observatory and data discovery resource: Data Science Journal, v. 8, IGY6-IGY20, accessed October 15, 2014, at https://www.jstage.jst.go.jp/article/dsj/8/0/8_SS_IGY-009/_article.

Scott, T.M., 2001, Text to accompany the geologic map of Florida: Florida Geological Survey Open-File Report 80, accessed July 7, 2014, at http://sofia.usgs.gov/publications/maps/florida_geology/OFR80.pdf.

Simpson, Fiona, and Bahr, Karsten, 2005, Practical magnetotelluric:, United Kingdom, Cambridge University Press, 272 p.

Smith, D.C., 1982, Review of the tectonic history of the Florida basement:Tectonophysics, v. 88, p. 1–22, accessed July 7, 2014, at http://www.sciencedirect.com/science/article/pii/0040195182902013.

Appendix

Table 1. Details of upper-bound model.

[km, kilometer; Ω•m, ohm meter; S/m, siemens per meter]

Layer	Depth (km)	Thickness (km)	Resistivity (Ω•m)	Conductivity (S/m)	Comments
1. Sedimentary section	[1] 0–1 km	1 km	[2] 900	0.0011	Resistivity values chosen using upper bound of old sediment range[2]
2. Crustal basement	[3] 1–40 km	39 km	[2] 10,000	0.0002	Resistivity values chosen from Jones, 1999[2]
3. Upper mantle	[4] 40–100 km	60 km	[5] 3,000	0.001	Resistivity value chosen from Mareschal and others, 1983, transect interpretation[5]
4. Upper mantle	[4] 100–250 km	150 km	138	[4] 0.005	Values correspond to John C. Stennis magnetic observatory[4]
5. Upper mantle	[4] 250–410 km	160 km	34	[4] 0.01	Values correspond to John C. Stennis magnetic observatory[4]
6. Transition zone	[4] 410–520 km	110 km	15.5	[4] 0.05	Values correspond to John C. Stennis magnetic observatory[4]
7. Transition zone	[4] 520–670 km	150 km	4.2	[4] 0.1778	Values correspond to John C. Stennis magnetic observatory[4]
8. Lower mantle	[4] 670–900 km	230 km	1.2	[6] 0.631	Values correspond to John C. Stennis magnetic observatory[4]
9. Lower mantle	[4] 900–1,000 km	100 km	0.87	[6] 1.12	Values correspond to John C. Stennis magnetic observatory[4]

[1] Barnett, 1975, table 1

[2] Jones, 1999, figure 1

[3] French and others, 2009, figure 2

[4] Kelbert and others, 2009, figure 2; global and regional resistivity model, North American regional resistivity chosen

[5] Mareschal and others, 1983

[6] Keller, 1966, table 10

Table 2. Details of lower-bound model.

[km, kilometer; Ω•m, ohm meter; S/m, siemens per meter]

Layer	Depth (km)	Thickness (km)	Resistivity (Ω•m)	Conductivity (S/m)	Comments
1. Sedimentary basin	[1] 0–6 km	6 km	[2] 5	0.2	[5] Resistivity values chosen from Keller
2. Crust	[3] 6–40 km	34 km	[5] 1,000	0.0001	[5] Resistivity values chosen from Keller
3. Upper mantle	[4] 40–100 km	60 km	[1] 50	0.0125	[1] Resistivity values chosen from Jones
4. Upper mantle	[4] 100–250 km	150 km	138	[4] 0.005	[4] Values correspond to Stennis magnetic observatory
5. Upper mantle	[4] 250–410 km	160 km	34	[4] 0.01	[4] Values correspond to John C. Stennis magnetic observatory
6. Transition zone	[4] 410–520 km	110 km	15.5	[4] 0.05	[4] Values correspond to John C. Stennis magnetic observatory
7. Transition zone	[4] 520–670 km	150 km	4.2	[4] 0.1778	[4] Values correspond to John C. Stennis magnetic observatory
8. Lower mantle	[4] 670–900 km	230 km	1.2	[4] 0.631	[4] Values correspond to John C. Stennis magnetic observatory
9. Lower mantle	[4] 900–1,000 km	100 km	0.87	[4] 1.12	[4] Values correspond to John C. Stennis magnetic observatory

[1] Barnett, 1975, table 1

[2] Jones, 1999, figure 1

[3] French and others, 2009, figure 2

[4] Kelbert and others (2009), figure 2, global and regional resistivity model, North American regional resistivity chosen

[5] Keller, 1966, table 10

Table 3. Details of geometric mean model.

[km, kilometer; Ω•m, ohm meter; S/m, siemens per meter]

Layer	Depth (km)	Thickness (km)	Resistivity (Ω•m)	Conductivity (S/m)
1. Sedimentary basin	0–1 km	1 km	67	0.01493
2. Sedimentary basin	1–6 km	5 km	224	0.00446
3. Crust	6–40 km	34 km	3,162	0.00032
4. Upper mantle	40–100 km	60 km	387	0.00258
5. Upper mantle	100–250 km	150 km	138	0.005
6. Upper mantle	250–410 km	160 km	34	0.01
7. Transition zone	410–520 km	110 km	15.5	0.05
8. Transition zone	520–670 km	150 km	4.2	0.1778
9. Lower mantle	670–900 km	230 km	1.2	0.631
10. Lower mantle	900–1,000 km	100 km	0.87	1.12